

## Research Article

# Comparison of Image Transform-Based Features for Visual Speech Recognition in Clean and Corrupted Videos

Rowan Seymour, Darryl Stewart, and Ji Ming

*School of Electronics, Electrical Engineering and Computer Science, Queen's University of Belfast, Belfast BT7 1NN, Northern Ireland, UK*

Correspondence should be addressed to Darryl Stewart, dw.stewart@qub.ac.uk

Received 28 February 2007; Revised 13 September 2007; Accepted 17 December 2007

Recommended by Nikos Nikolaidis

We present results of a study into the performance of a variety of different image transform-based feature types for speaker-independent visual speech recognition of isolated digits. This includes the first reported use of features extracted using a discrete curvelet transform. The study will show a comparison of some methods for selecting features of each feature type and show the relative benefits of both static and dynamic visual features. The performance of the features will be tested on both clean video data and also video data corrupted in a variety of ways to assess each feature type's robustness to potential real-world conditions. One of the test conditions involves a novel form of video corruption we call *jitter* which simulates camera and/or head movement during recording.

Copyright © 2008 Rowan Seymour et al. This is an open access article distributed under the Creative Commons Attribution License, which permits unrestricted use, distribution, and reproduction in any medium, provided the original work is properly cited.

## 1. INTRODUCTION

Speech is one of the most natural and important means of communication between people. Automatic speech recognition (ASR) can be described as the process of converting an audio speech signal into a sequence of words by computer. This allows people to interact with computers in a way which may be more natural than through interfaces such as keyboards and mice, and has already enabled many real-world applications such as dictation systems and voice controlled systems. A weakness of most modern ASR systems is their inability to cope robustly with audio corruption which can arise from various sources, for example, environmental noises such as engine noise or other people speaking, reverberation effects, or transmission channel distortions caused by the hardware used to capture the audio signal. Thus one of the main challenges facing ASR researchers is how to develop ASR systems which are more robust to these kinds of corruptions that are typically encountered in real-world situations. One approach to this problem is to introduce another modality to complement the acoustic speech information which will be invariant to these sources of corruption.

It has long been known that humans use available visual information when trying to understand speech, especially in noisy conditions [1]. The integral role of visual information in speech perception is demonstrated by the McGurk effect [2], where a person is shown a video recording of one phoneme being spoken, but the sound of a different phoneme being spoken is dubbed over it. This often results in the person perceiving that he has heard a third intermediate phoneme. For example, a visual /ga/ combined with an acoustic /ba/ is often heard as /da/. A video signal capturing a speaker's lip movements is unaffected by the types of corruptions outlined above and so it makes an intuitive choice as a complementary modality with audio.

Indeed, as early as 1984, Petajan [3] demonstrated that the addition of visual information can enable improved speech recognition accuracy over purely acoustic systems, as visual speech provides information which is not always present in the audio signal. Of course it is important that the new modality provides information which is as accurate as possible and so there have been numerous studies carried out to assess and improve the performance of visual speech recognition. In parallel with this, researchers have been investigating effective methods for integrating the two

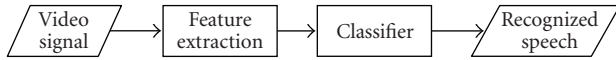


FIGURE 1: The general process of automatic speech recognition.

modalities so that maximum benefit can be gained from their combination.

A visual speech recognition system is very similar to a standard audio speech recognition system. Figure 1 shows the different stages of the typical recognition process. Before the recognition process can begin, the speech models must be constructed. This is usually performed by analyzing a training set of suitable video examples, so that the model parameters for the speech units can be estimated. The speech models are usually *hidden Markov models* (HMM) or *artificial neural networks* (ANN). Once the models are constructed, the classifier can use them to calculate the most probable speech unit when given some input video.

Visual features will usually be extracted from the video frames using a process similar to that shown in Figure 2. Depending on the content of the video (i.e., whether it contains more than one speaker's face), it may be necessary to start with a face detection stage which returns the most likely location of the speaker's face in the video frame. The consecutive stages of face localization and mouth localization provide a cropped image of the speaker's mouth.

The lip parameterization stage may be geometric based or image transform based. Petajan's original system [3] is an example of geometric-based feature extraction which used simple thresholding of the mouth image to highlight the lip area, and then measurements of mouth height, width, and area were taken from that. Since then, many approaches have been developed which exploit our knowledge of the shape of a human mouth to fit more complex models to speakers' mouths. These methods include *active contours* (often referred to as *snakes*) [4], *deformable templates* [5–10], *active shape models* [11], and various other approaches [12–14].

Whereas geometric methods utilize knowledge of the structure of the human mouth to extract features which describe its shape, image transform methods attempt to transform the image pixel values of each video frame into a new lower-dimensional space, which removes redundant information and provides better class discrimination. As with geometric-based approaches, there have also been numerous studies using different image transform methods. These methods include discrete cosine transform (DCT) [15–18], discrete wavelet transform (DWT) [15, 19], principal component analysis (PCA) [4, 15, 20], and linear discriminant analysis (LDA) [21].

In [15], Potamianos et al. give a comparison of DCT, DWT, Walsh, Karhunen-Loève transform (KLT), and PCA transforms and conclude that the DWT and DCT transforms are preferable to other transforms, such as PCA, which require training. They also tested the features under several noisy video conditions including video field rate decimation, additive white noise, and JPEG image compression and showed that image transform-based features are quite robust

to these conditions. In this paper, we wish to carry out a complementary study in which we will compare the performance of a variety of different image transform-based feature types for speaker-independent visual speech recognition of isolated digits recorded in various noisy video conditions which may occur in real-world operating conditions. This work extends upon our previous research on the use of geometric-based features for audio-visual speech recognition subject to both audio and video corruptions [22].

Specifically, we will compare the performance of features extracted using the discrete cosine transform (DCT), discrete wavelet transform (DWT), principal component analysis (PCA), linear discriminant analysis (LDA), and fast discrete curvelet transform (FDCT). This will be the first reported results of a system which uses FDCT features for visual speech recognition. The video corruptions used in our tests include video blurring, video compression, and a novel form of video noise we call *jitter* which is designed to simulate the corrupting effects of either camera movement/vibration or the tilting/movement of the speaker's head while speaking. For each of the transforms, we will investigate various parameters which could affect their performance, such as the feature selection method for DCT features and the wavelet base and decomposition levels for DWT features. We also investigate the performance improvement gained by augmenting static visual features with their associated dynamic features.

In our experiments, we will be carrying out speaker-independent isolated digit recognition tests using a large internationally standard database and while these experiments will not show the absolute performance which would be achieved on all other recognition tasks or databases, they should allow judgments to be made about the expected comparative performance of the feature types on new data.

This paper is organized as follows. In Section 2, the image transform feature types used in this work are discussed. Section 3 outlines the preparation of the video data used in experiments. Section 4 contains the experimental results and discussion. Finally in Section 5, a summary is provided of the main findings and conclusions which can be drawn from the results.

## 2. IMAGE TRANSFORM TYPES

As was stated above, we will be comparing the performance of five different image transform-based feature types. These are DCT, DWT, PCA, LDA, and finally FDCT. The first four of these are well known in the literature so we will not describe them again here. Instead, we refer the interested reader to descriptions which can be found in [23]. However, the FDCT is less well known, so a description is provided in the next subsection.

### 2.1. Fast discrete curvelet transform

The curvelet transform is a relatively new multiscale transform introduced and described in detail in [24]. The motivation for the development of the new transform was to find a

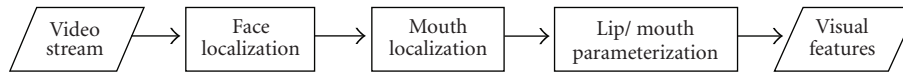


FIGURE 2: The general process of visual feature extraction.

way to represent edges and other singularities along curves in a way that was more efficient than existing transforms, that is, less coefficients are required to reconstruct an edge to a given degree of accuracy. Like the wavelet transform, the curvelet transform uses frame elements indexed by scale and location, but unlike the wavelet transform it also uses directional parameters. The transform is based on an anisotropic scaling principle, unlike the isotropic scaling principle of the wavelet transform.

Theoretically, therefore, such a transform may be able to extract information about a speaker’s lip contour more efficiently than the DCT or DWT. In [25], two implementations of the curvelet transform for digital signals are described: one using unequid spaced fast Fourier transforms (FFTs) and another using frequency wrapping. These transforms are referred to as *fast discrete curvelet transforms*. The MATLAB toolkit *CurveLab* [26] was used to implement an FDCT (using unequid spaced FFTs) in this work.

### 3. EXPERIMENTAL DATA

#### 3.1. XM2VTS database

For this work we used the XM2VTS database [27]. This database contains 295 speakers, roughly balanced between genders. Each speaker was recorded saying all ten digits four times in four different sessions in a quiet environment. The data was divided into 200 speakers for training and 95 speakers for testing. Thus, there were 3200 training occurrences of each digit and the test data includes 15200 test tokens. This provides sufficient data to train speaker-independent digit models. The data is supplied as continuous digit sequences with only sentence-level transcriptions. However, as was stated previously, for this work we decided to carry out isolated digit recognition experiments, so a forced alignment procedure was initially carried out on all utterances using the hidden Markov toolkit (HTK) [11] in order to obtain word boundary positions. The database is also supplied with lip tracking results, using the color-based approach described by Ramos Sanchez [28]. These were used to localize the mouth region of interest (ROI) in each video frame.

#### 3.2. Video noise

Three different types of noise were considered which represent corruption likely to occur in a real-world application: compression, blurring, and jitter (see Figure 3).

##### 3.2.1. Compression

Video that is being streamed over a network where bandwidth is constrained, or stored on a computer where storage



FIGURE 3: From left to right: an original video frame, the same frame compressed (MPEG4 at 4 Kbps), blurred with a Gaussian filter with a standard deviation of 12, and with jitter level 12 applied.

space may be limited, is usually compressed using a codec. Most modern mobile phones are capable of recording and transmitting video recordings, and these are normally highly compressed to reduce bandwidth requirements. The MPEG4 codec was used as it is a modern and popular format, used commonly for sharing files on the Internet. Each video file in the test set was compressed to 7 different levels of bitrate, that is, 512, 256, 128, 64, 32, 16, 8, 4 Kbps.

##### 3.2.2. Blurring

Image blurring represents real-world situations where the video camera loses focus on the speaker (many webcams must be manually focused) or situations where the speaker is far away from the camera. In such a situation, the portion of the video frame containing the speaker’s mouth will be very small and may have to be interpolated to a higher resolution to work with a lip feature extraction system. The test videos were blurred using Gaussian filters with 7 different standard deviation values, that is, 4, 8, 12, 16, 20, 24, 28.

##### 3.2.3. Jitter

Jitter represents either camera shake, supposing the camera is not mounted securely, or problems with the accurate tracking and centering of the mouth when the speaker’s head is moving. In a real-world application, it is unlikely that a user would keep his head as still as the subjects in our data, so it is assumed that the tracking of the mouth ROI would not be as smooth when his head is moving. Jitter is applied by taking each clean video frame and adding a random variation to the coordinates and orientation of the mouth ROI. The new resulting video gives the impression that the speakers mouth is shifting and rotating randomly at each frame inside the ROI. Different levels of jitter are generated by scaling the random variation. For example, jitter level 10 corresponds to a random rotation in the range  $[-10^\circ, 10^\circ]$  and separate random translations along the  $x$  and  $y$  axes, both in the range  $[-10, 10]$  pixels. Six jitter levels were used on the test video data, that is, 2, 4, 6, 8, 10, 12.

For all 3 methods, the corruption levels used were chosen to produce a good range of recognition accuracies from approximately random to optimal.

## 4. EXPERIMENTS

The following experiments all involve speaker-independent digit recognition. The HMM models consisted of 10 states per digit, with each state represented by Gaussian mixture models with 4 mixtures. For all experiments, the models were trained using noise-free video data from 200 subjects, and tested using the data from the remaining 95 subjects.

Prior to each of the image transforms, the mouth ROI in each video frame is converted to the YUV colorspace and only the Y channel is kept, as this retains the image data least effected by the video compression. This was cropped by a fixed amount, subsampled, and then passed as the input to the image transforms.

### 4.1. Transform parameters

Some preliminary experiments were performed to determine the appropriate image resolution for input to the image transforms, and it was found that images of  $16 \times 16$  pixels (as used in [15, 16]) provided slightly better performance than  $32 \times 32$  pixel images, so we used the  $16 \times 16$  pixel images here.

In some previous studies using DCT features, the DC component (i.e., the first component) is excluded [16] but in others it is retained [15]. Preliminary experiments showed that including the DC component gave slightly improved recognition performance, so we have included it in all our DCT-based experiments.

Further, preliminary experiments specific to the DWT-based features were carried out to identify which type of wavelet was most effective, that is, which wavelet base and level of decomposition are appropriate. The Haar wavelet, two Daubechies wavelets (D4 and D6) [29], and the Antonini wavelet [30] were examined. The two Daubechies wavelets were selected because they had been shown to perform well for lip reading by previous researchers [19]. The Antonini wavelet was chosen because it is commonly used for image compression, and is well known for being used by the FBI for compressing fingerprint images [31]. We found that although there was only a small variation in the performance of these alternatives, the wavelet base and decomposition level that performed the best were those of the Daubechies 4 wavelet, with 3 levels of decomposition (filter coefficients [0.483, 0.837, 0.224, -0.129]). Hence, this was used in all the subsequent experiments, and is what we imply by *DWT* from here on.

A final postprocessing step applied in feature extraction systems is feature normalization. This is especially important in speaker-independent systems where interspeaker variability must be modeled. Many systems employ *mean subtraction* to achieve this normalized state, whereby the mean for each feature is calculated over the utterance, and then subtracted from that feature in every frame. This was the normalization method we employed.

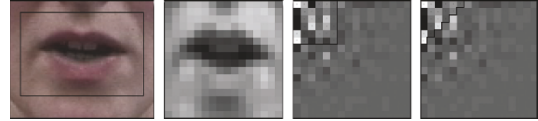


FIGURE 4: From left to right: original lip image, subsampled  $16 \times 16$  ROI, DCT coefficients with square  $6 \times 6$  selection, and with triangle  $6 \times 6$  selection.

### 4.2. Comparison of feature set selection methods

The purpose of feature selection is to extract from the coefficients generated by an image transform a new set of values which are suitable for recognition, that is, they have good class discrimination and suitably low dimensionality. The number of coefficients is usually proportional to the processing time required by a recognition system to train models or recognize data. Some feature selection methods are appropriate for some kinds of image transform, but inappropriate for others.

The simplest type of feature selection is a fixed 2D mask. The DCT and DWT transforms return a 2D matrix of coefficients, and so coefficients can be selected from the parts of those matrices which contain the most useful information. Both transforms place the lowest frequency information in the upper-left corner of the matrix, so extracting the coefficients within a square aligned with the upper-left corner of the matrix (see Figure 4) provides a set of low-frequency coefficients suitable for recognition. The DCT coefficients, however, are packed by ascending frequency in diagonal lines so a triangle selection may be more appropriate.

For the DCT, both square and triangular 2D masks were compared. Figure 5 shows speech recognition results in word error rate (WER) using these feature selection methods with DCT coefficients. At this stage only static features were used to allow their selection to be optimized before introducing dynamic features. Each feature selection method was used to generate different sizes of final feature vector to show the optimum feature vector size for each method. As expected, the triangle mask outperformed the square mask, as this includes more of the coefficients corresponding to low frequencies.

For the DWT it does not make sense to extract coefficients using a triangular mask, because they are organized in squares, so only square mask selection was considered. Though the coefficients are packed into squares whose widths and heights are  $2^N$  (where  $N$  is an integer), square masks of any integer size were tried for completeness. Figure 5 shows the performance the DWT coefficients with square selection of features. The DWT coefficients were generated using the Daubechies 4 wavelet with 3 levels of decomposition, as this was found to be optimal in Section 4.1.

The best performance result was found for a square mask of size  $8 \times 8$ , which corresponds to all the detailed coefficients of the 2nd and 3rd levels of decomposition, as well as the approximation coefficients of the 3rd. The number of 64 static features, however, is a very large number before dynamic features have even been considered. The DWT features are not included in subsequent experiments as they required a much

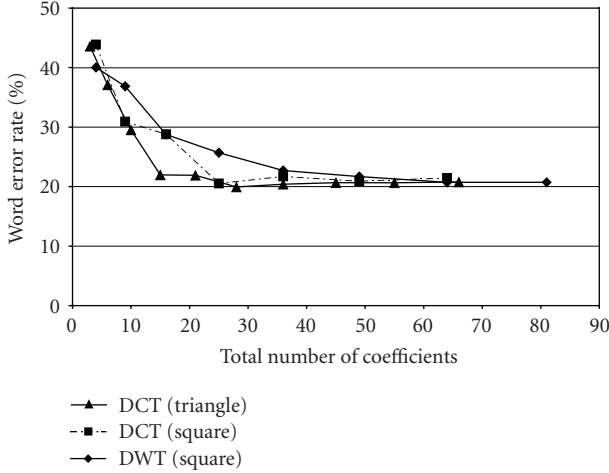


FIGURE 5: Recognition performance using different feature selection methods applied to static DCT and DWT coefficients.

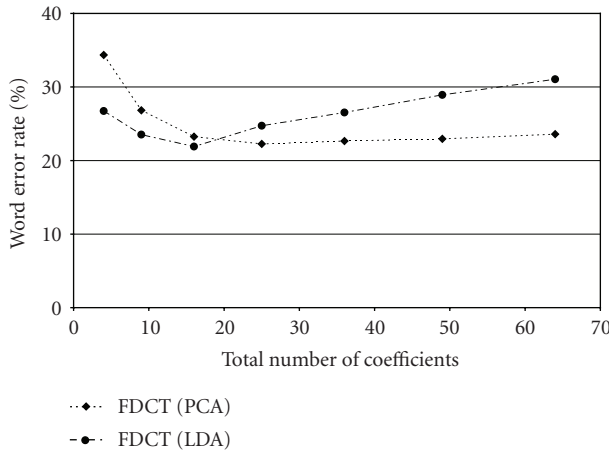


FIGURE 6: Recognition performance using different feature selection methods applied to static FDCT coefficients.

higher number of coefficients to achieve similar accuracy to the other feature types.

The coefficients produced by the FDCT have a very high dimensionality (2752) and are not organized in such a way that it would make sense to use a 2D mask such as a triangle or square. Because the FDCT is a nonlinear transformation, it is appropriate to apply one of the linear data compression transformations (PCA or LDA) in order to reduce the high-dimensional coefficients to low-dimensional features. The results of using both of those transformations on FDCT coefficients are shown in Figure 6. LDA outperformed PCA for low numbers of coefficients (less than 20). For higher numbers of coefficients, PCA outperformed LDA, but the best result for any number was 21.90% for LDA with 16 coefficients, making LDA the optimum selection method for FDCT coefficients.

PCA and LDA were also used as first-stage image transformations (Figure 7) by using the raw mouth images (sub-

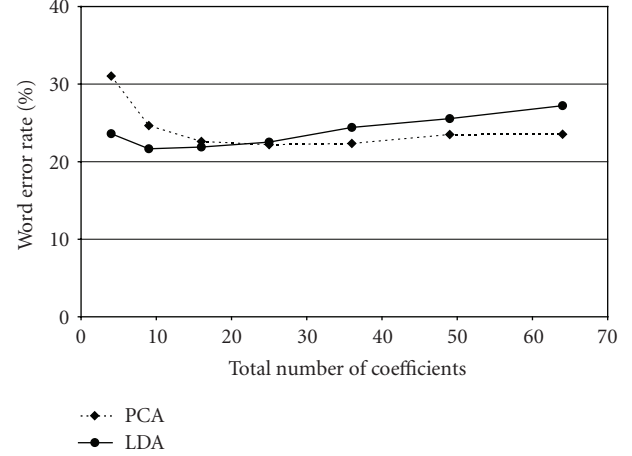


FIGURE 7: Recognition performance using PCA and LDA transformations of raw images to generate static features.

TABLE 1: Average (absolute) reduction in WER achieved using (static +  $\Delta$ ) features compared to (static only) features and (static +  $\Delta$  +  $\Delta\Delta$ ) features compared to (static +  $\Delta$ ) features.

Image transform	(Static + $\Delta$ ) versus (static only)	(Static + $\Delta$ + $\Delta\Delta$ ) versus (static + $\Delta$ )
DCT	12.9%	1.5%
FDCT	8.7%	0.8%
PCA	9.4%	0.8%
LDA	8.1%	0.6%

sampled to  $16 \times 16$ ) as inputs instead of coefficients from other transformations. The coefficients returned from the PCA and LDA transformations are ordered by significance, and so a feature set with  $k$  features is formed by simply taking the first  $k$  coefficients. Mirroring what was found for FDCT coefficients, for approximately less than 20 coefficients, LDA performed best, but for higher numbers, PCA performed best.

### 4.3. Dynamic features

Dynamic features provide information about the change or rate of change of the static features over time. It is well known in acoustic-based speech recognition that dynamic features provide valuable discriminative information. In this work, we wished to assess the value of dynamic features in the visual speech domain. The dynamic features we use in these experiments were calculated as the first and second derivatives of cubic splines constructed for each feature in each utterance. We use  $\Delta$  to denote the first derivative features (amount of change) and  $\Delta\Delta$  to denote the second derivative features (rate of change). The final feature vector is formed by concatenating the static and dynamic features.

We compared the performance of feature vectors covering a range of sizes which included combinations of static and dynamic features generated using each of the transforms

TABLE 2: Summary of WERs achieved on clean video using the optimal feature vectors extracted from each image transform.

Image transform	DCT	FDCT	PCA	LDA
Selection method	Triangle	LDA	—	—
Vector size	30	18	50	18
WER (%)	12.11	14.64	13.43	13.65

discussed in the previous sections. It can be seen in Table 1 that in all cases the introduction of  $\Delta$  features provides a substantial average improvement in WER compared to using only static features. However, the further addition of  $\Delta\Delta$  features provides only a small extra improvement whilst requiring a 50% increase in the feature vector size. Therefore, we decided to use only static +  $\Delta$  features in our next series of experiments.

Table 2 summarizes the recognition performance achieved on clean video for each feature type using the best feature selection method for that type (as chosen in Section 4.2) and the feature vector size (consisting of static features augmented with their  $\Delta$  dynamic features) which we found to give the best accuracy.

The overall accuracy of the recognition system is affected by the vocabulary size and the visual similarity of the words which are in the vocabulary. As the vocabulary size is increased, there are more units which need to be distinguished and hence be more potential for errors to be made. However, it is the visual similarity of words which causes recognition errors, so if the vocabulary of a system is increased but includes words which are much more visibly distinct, then it is likely that the accuracy would improve rather than deteriorate. For instance, if the size of the vocabulary was only two words, then the potential for error is much reduced compared to the ten-word vocabulary for digit recognition. However, if the two-word vocabulary includes just the words “pet” and “bet,” then the accuracy of the system is likely to be very poor because these two words are virtually indistinguishable visually. By examining the confusion matrices generated in our recognition experiments, we can see which digits are most easily recognized and which are most confusable. The confusion matrix for DCT features from clean video showed that the digit recognized correctly most often was “one” and the digit recognized incorrectly most often was “nine.” Specifically, the most common mistake made was a “nine” being incorrectly recognized as a “six.” Although “nine” and “six” are acoustically very different, they actually involve similar lip movements and hence appear similar to a lip reading system.

#### 4.4. Robustness to video corruption

The recognition performance of the optimal feature vectors for each feature type was compared using the video corruption types described in Section 3.1. For video compression

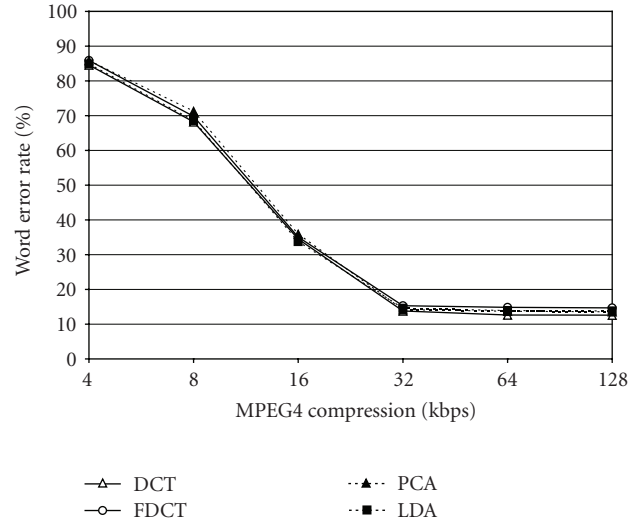


FIGURE 8: WERs achieved using optimal feature vectors for different feature types on video data compressed at various levels of MPEG4 video compression.

(Figure 8) it can be seen that all of the feature types perform similarly and that they are affected in a uniform way by increased video compression. We think that the similarity in performance can be explained by the fact that this kind of video compression causes corruption mainly to the temporal information in the video. The compression algorithm uses keyframes which means that some video frames will be stored with little loss of information, but that subsequent frames may repeat this information (appearing as frozen frames). Thus, a frame may appear as uncorrupted, and generate the same features as a clean frame, but those features will represent an incorrect state when being recognized by the HMM. This seems to indicate that in order to improve recognition rates for visual speech recognition on compressed video a new modeling and recognition approach would be needed which can deal with the occurrence of skipped/frozen frames rather than a new type of visual feature. The performances of all our tested systems are quite stable until the bitrate drops below 32 Kbps. This would indicate a minimum reliable operating constraint on the input video for our standard HMM-based models.

For video frame blurring (Figure 9) all of the feature types show good robustness, even at high levels where it would be very difficult for a human to comprehend the content of the video. There is more difference between the performance of the feature types here than in video compression, but DCT provides the best WER, as was also true for the video compression experiments, albeit, to a lesser degree. This is possibly to be expected as feature types which emphasize that low-frequency information (such as the DCT) should be the most robust to blurring, which essentially destroys high-frequency information and leaves low-frequency information intact.

In contrast, for video frame jitter (Figure 10), the DCT performs worst in almost all tested levels of corruption,

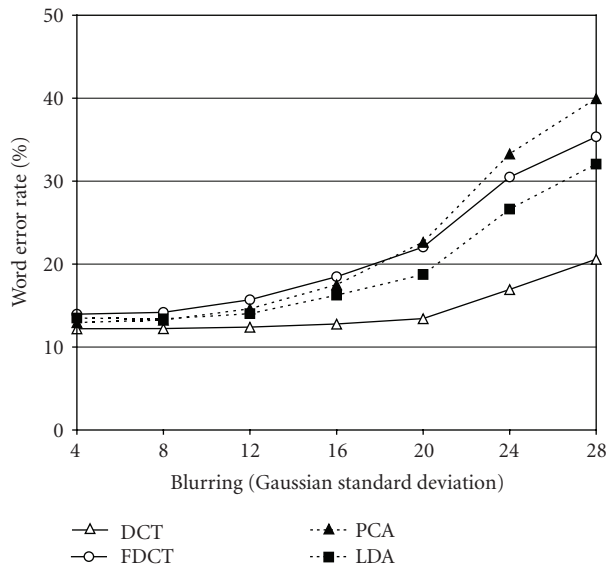


FIGURE 9: WERs achieved using optimal feature vectors for different feature types on video data at various levels of video frame blurring.

showing its high sensitivity and fragility to motion. PCA performs worst at the highest levels of corruption and overall, the LDA transform performs the best with jitter, though for the highest levels, the FDCT performs the best. However, the performance of all of the feature types deteriorates quickly in the presence of even moderate levels of this type of corruption, which shows the importance of robust video preprocessing methods which can make corrections for translation and rotation of the mouth ROI, similar to the rotation correction used in [16].

## 5. SUMMARY

In this paper, the performances of several image transform-based feature extraction methods were compared for visual speech recognition in clean and noisy video conditions. This included the first reported results using FDCT-based features. We have compared feature set selection methods for some of the feature types and suggested the optimal method in each case.

It was hoped that the FDCT would be able to capture important and useful information about the speakers lip contour which would not be captured by the more commonly used DCT and DWT transforms. However, the recognition results in our experiments show that although the performance is similar, it does not provide any improvement. It may be the case that the FDCT method captures more *speaker* specific information rather than *speech* information and therefore may be a suitable feature type for use in visual *speaker* recognition systems. Furthermore, in this paper we used the PCA and LDA transforms to select features from the FDCT coefficients; however, alternative methods do exist which could be used instead of these such as select-

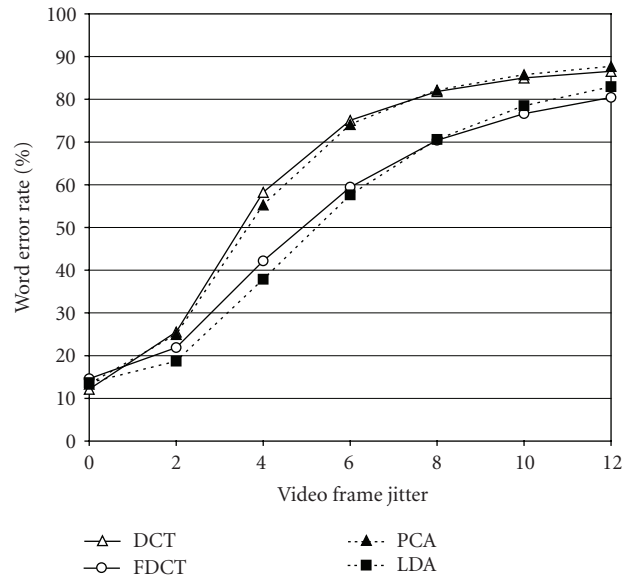


FIGURE 10: WERs achieved using optimal feature vectors for different feature types on video data corrupted at various levels of video frame jitter.

ing coefficients with the highest energy or variance as suggested in [32] and these could perhaps provide some improvement.

We have also investigated the relative merit of augmenting the features with their associated dynamic features and found that in clean recognition conditions a substantial improvement in recognition accuracy was gained by using  $\Delta$  dynamic features but that only a small additional benefit was achieved through the introduction of  $\Delta\Delta$  dynamic features. However, it is possible that the main benefits of using  $\Delta\Delta$  dynamic features would be seen when testing in noisy rather than in clean conditions and this could be investigated in the future.

A series of experiments were used to test the robustness of the feature types to different forms and levels of video noise. Specifically, tests were performed on video which was subject to compression, blurring, and a novel form of video corruption, called “jitter,” which simulated camera shake or head movement. It was found that video compression degrades the performance of all the tested features in a uniform manner. We suggest that improving the HMM modeling approach to cater for frozen video frames would be a possible method of dealing with this type of corruption. Jitter corruption was shown to have a strong negative effect on the performance of the tested features, even at quite low levels of jitter, which demonstrates the importance of robust and accurate video preprocessing methods to ensure that the mouth ROI is correctly aligned for a visual speech recognition system. From the tests on blurred video, it was shown that the tested feature types are quite robust to this form of corruption and that the DCT transform in particular was very robust even at levels of blurring where the content of the video data would be incomprehensible to a human.

## ACKNOWLEDGMENTS

The authors thank the reviewers for their helpful comments. This work was supported by the UK EPSRC under Grant EP/E028640/1 ISIS.

## REFERENCES

- [1] W. G. Sumbly and I. Pollack, "Visual contribution to speech intelligibility in noise," *Journal of Acoustical Society of America*, vol. 26, no. 2, pp. 212–215, 1954.
- [2] H. McGurk and J. MacDonald, "Hearing lips and seeing voices," *Nature*, vol. 264, no. 5588, pp. 746–748, 1976.
- [3] E. D. Petajan, *Automatic lipreading to enhance speech recognition*, Ph.D. thesis, University of Illinois, Urbana-Champaign, Ill, USA, 1984.
- [4] C. Bregler and Y. Konig, "'Eigenlips' for robust speech recognition," in *Proceedings of IEEE International Conference on Acoustics, Speech, and Signal Processing (ICASSP '94)*, vol. 2, pp. 669–672, Adelaide, SA, Australia, April 1994.
- [5] A. L. Yuille and P. W. Hallinan, "Deformable templates," in *Active Vision*, pp. 21–38, MIT Press, Cambridge, Mass, USA, 1993.
- [6] M. E. Hennecke, K. V. Prasad, and D. G. Stork, "Using deformable templates to infer visual speech dynamics," Tech. Rep., California Research Center, Menlo Park, Calif, USA, 1994.
- [7] S. Horbelt and J. Dugelay, "Active contours for lipreading—combining snakes with templates," in *Proceedings of the 15th GRETSI Symposium on Signal and Image Processing*, pp. 717–720, Juan-Les-Pins, France, September 1995.
- [8] M. Vogt, "Fast matching of a dynamic lip model to color video sequences under regular illumination conditions," in *Speechreading by Humans and Machines*, vol. 150, pp. 399–408, Springer, New York, NY, USA, 1996.
- [9] T. Coianiz, L. Torresani, and B. Caprile, "2d deformable models for visual speech analysis," in *Speechreading by Humans and Machines*, vol. 150, pp. 391–398, Springer, New York, NY, USA, 1996.
- [10] D. Chandramohan and P. L. Silsbee, "A multiple deformable template approach for visual speech recognition," in *Proceedings of the 4th International Conference on Spoken Language Processing (ICSLP '96)*, vol. 1, pp. 50–53, Philadelphia, Pa, USA, October 1996.
- [11] J. Luetttin, N. A. Thacker, and S. W. Beet, "Active shape models for visual speech feature extraction," in *Speechreading by Humans and Machines*, vol. 150, pp. 383–390, Springer, New York, NY, USA, 1996.
- [12] R. Kaucic, B. Dalton, and A. Blake, "Real-time lip tracking for audio-visual speech recognition applications," in *Proceedings of the 4th European Conference on Computer Vision (ECCV '96)*, vol. 1065, pp. 376–387, Cambridge, UK, April 1996.
- [13] M. Gordan, C. Kotropoulos, and I. Pitas, "Pseudoautomatic lip contour detection based on edge direction patterns," in *Proceedings of the 2nd International Symposium on Image and Signal Processing and Analysis (ISPA '01)*, pp. 138–143, Pula, Croatia, June 2001.
- [14] R. Goecke, J. B. Millar, A. Zelinsky, and J. Robert-Ribes, "A detailed description of the AVOZES data corpus," in *Proceedings of IEEE International Conference on Acoustics, Speech, and Signal Processing (ICASSP '01)*, pp. 486–491, Salt Lake City, Utah, USA, May 2001.
- [15] G. Potamianos, H. P. Graf, and E. Cosatto, "An image transform approach for HMM based automatic lipreading," in *Proceedings of the International Conference on Image Processing (ICIP '98)*, vol. 3, pp. 173–177, Chicago, Ill, USA, October 1998.
- [16] E. Patterson, S. Gurbuz, Z. Tufekci, and J. Gowdy, "CUAVE: a new audio-visual database for multimodal human-computer-interface research," in *Proceedings of IEEE International Conference on Acoustics, Speech, and Signal Processing (ICASSP '02)*, vol. 2, pp. 2017–2020, Orlando, Fla, USA, May 2002.
- [17] P. Císař, M. Železný, J. Zelinka, and J. Trojanová, "Development and testing of new combined visual speech parameterization," in *Proceedings of the International Conference on Auditory-Visual Speech Processing (AVSP '07)*, Hilvarenbeek, The Netherlands, August–September 2007.
- [18] M. Heckmann, K. Kroschel, C. Savariaux, and F. Berthommier, "DCT-based video features for audio-visual speech recognition," in *Proceedings of the 7th International Conference on Spoken Language Processing (ICSLP '02)*, pp. 1925–1928, Denver, Colo, USA, September 2002.
- [19] I. Matthews, G. Potamianos, C. Neti, and J. Luetttin, "A comparison of model and transform-based visual features for audio-visual LVCSR," in *Proceedings of IEEE International Conference on Multimedia and Expo (ICME '01)*, pp. 825–828, Tokyo, Japan, August 2001.
- [20] L. Révéré, "From raw images of the lips to articulatory parameters: a viseme-based prediction," in *Proceedings of the 5th European Conference on Speech Communication and Technology (EuroSpeech '97)*, vol. 4, pp. 2011–2014, Rhodes, Greece, September 1997.
- [21] G. Potamianos and H. P. Graf, "Linear discriminant analysis for speechreading," in *Proceedings of 2nd IEEE Workshop on Multimedia Signal Processing (MMSP '98)*, pp. 221–226, Redondo Beach, Calif, USA, December 1998.
- [22] R. Seymour, J. Ming, and D. Stewart, "A new posterior based audio-visual integration method for robust speech recognition," in *Proceedings of the 9th European Conference on Speech Communication and Technology (InterSpeech '05)*, pp. 1229–1232, Lisbon, Portugal, September 2005.
- [23] A. K. Jain, *Fundamentals of Digital Image Processing*, Prentice-Hall, Englewood Cliffs, NJ, USA, 1989.
- [24] E. J. Candés and D. L. Donoho, "Curvelets—a surprisingly effective nonadaptive representation for objects with edges," in *Curve and Surface Fitting*, A. Cohen, C. Rabut, and L. L. Schumaker, Eds., Vanderbilt University Press, Nashville, Tenn, USA, 1999.
- [25] E. J. Candés, L. Demanet, D. L. Donoho, and L. Ying, "Fast discrete curvelet transforms," Tech. Rep., California Institute of Technology, Pasadena, Calif, USA, 2005.
- [26] E. J. Candés, L. Demanet, and L. Ying, *CurveLab Toolbox*, 2005.
- [27] K. Messer, J. Matas, J. Kittler, J. Luetttin, and G. Maitre, "XM2VTSDB: the extended M2VTS database," in *Proceedings of the 2nd International Conference on Audio- and Video-Based Biometric Person Authentication (AVBPA '99)*, pp. 72–77, Washington, DC, USA, March 1999.
- [28] M. U. Ramos Sanchez, *Aspects of facial biometrics for verification of personal identity*, Ph.D. thesis, The University of Surrey, Guilford, UK, 2000.
- [29] I. Daubechies, *Ten Lectures on Wavelets*, SIAM, Philadelphia, Pa, USA, 1992.

- 
- [30] M. Antonini, M. Barlaud, P. Mathieu, and I. Daubechies, "Image coding using wavelet transform," *IEEE Transactions of Image Processing*, vol. 1, no. 2, pp. 205–220, 1992.
  - [31] C. M. Brislawn, "The FBI fingerprint image compression specification," in *Wavelet Image and Video Compression*, chapter 16, pp. 271–288, Kluwer Academic Publishers, Dordrecht, The Netherlands, 1998.
  - [32] M. Heckmann, F. Berthommier, and K. Kroschel, "Noise adaptive stream weighting in audio-visual speech recognition," *EURASIP Journal on Applied Signal Processing*, vol. 2002, no. 11, pp. 1260–1273, 2002.